CHEMICAL ENGINEERING

Kilogram-scale prexasertib monolactate monohydrate synthesis under continuous-flow CGMP conditions

Kevin P. Cole,[1]* Jennifer McClary Groh,[1] Martin D. Johnson,[1] Christopher L. Burcham,[1] Bradley M. Campbell,[1] William D. Diseroad,[2] Michael R. Heller,[1] John R. Howell,[1] Neil J. Kallman,[1] Thomas M. Koenig,[3] Scott A. May,[1] Richard D. Miller,[1] David Mitchell,[1] David P. Myers,[1] Steven S. Myers,[1] Joseph L. Phillips,[1] Christopher S. Polster,[1] Timothy D. White,[1] Jim Cashman,[4] Declan Hurley,[5] Robert Moylan,[5] Paul Sheehan,[5] Richard D. Spencer,[6] Kenneth Desmond,[7] Paul Desmond,[7] Olivia Gowran[7]

Advances in drug potency and tailored therapeutics are promoting pharmaceutical manufacturing to transition from a traditional batch paradigm to more flexible continuous processing. Here we report the development of a multistep continuous-flow CGMP (current good manufacturing practices) process that produced 24 kilograms of prexasertib monolactate monohydrate suitable for use in human clinical trials. Eight continuous unit operations were conducted to produce the target at roughly 3 kilograms per day using small continuous reactors, extractors, evaporators, crystallizers, and filters in laboratory fume hoods. Success was enabled by advances in chemistry, engineering, analytical science, process modeling, and equipment design. Substantial technical and business drivers were identified, which merited the continuous process. The continuous process afforded improved performance and safety relative to batch processes and also improved containment of a highly potent compound.

A trend has emerged within small-molecule pipelines of the pharmaceutical industry of investigational medicines, which have lower projected volumes relative to historical small-molecule drugs due to increased potency and smaller targeted patient populations (*1*–*3*). Highly potent compounds require high levels of operational containment to avoid exposure to plant personnel and particular attention to equipment cleaning to avoid cross-contamination with other materials. As these products move through development, they pose a challenge to the current batch manufacturing infrastructure of large (≥4 m^3) reactors within many pharmaceutical companies. Batch pharmaceutical manufacturing has remained mostly unchanged for many decades and relies on large, fixed, and costly equipment sets, which are often grossly oversized for newer products. This mismatch in process scale versus market volume necessitates new capital expenditures for appropriately sized production sites. Small-volume continuous (SVC) manufacturing encompasses small-scale (3 to 15 kg/day) production in a flexible environment (*4*, *5*). Operation in fume hoods reduces the necessary capital investment, as equipment does not need to be explosion proof, and continuous-flow apparatuses offer expanded processing space under safe conditions. For products requiring stringent cleaning, equipment sets can be dedicated to that product or disposable due to the low replacement cost. Perhaps the greatest opportunity afforded by SVC manufacturing is the ability to rapidly produce active pharmaceutical ingredients (APIs) on-demand, which allows substantial inventory reduction and may provide financial and supply chain benefits, especially if the drug substance is linked to the final formulated product (*6*).

Although common in the manufacture of petrochemicals, food, and fine chemicals, continuous manufacturing (CM) has only recently gained substantial attention within pharma for low-volume products (*7*, *8*). The U.S. Food and Drug Administration has advocated for the modernization of pharmaceutical manufacturing and is supportive of CM methods, which offer numerous advantages over batch processes, such as expanded processing space enabled by extreme conditions, as well as improved product quality due to increased use of process analytical technology (PAT) and quality by design (*9*–*12*). Additional processing benefits from advanced manufacturing methods may also be realized; these include reduced waste generation, the ability to safely process high-energy intermediates, and decreased energy consumption (*13*). The Defense Advanced Research Projects Agency (DARPA) investigated miniaturization of API production and mobile on-demand CM plants (*14*). There are many examples of continuous production of APIs but few that adopt current good manufacturing practices (CGMP) (*15*–*17*). Many pharmaceutical CM examples comprise only chemical transformations, with separations such as crystallization or extraction performed in batch mode. In recent years, publications from various research groups have reported multistep continuous processes and on-demand proof-of-concept work with little to no description of a suitable control strategy. CM has been demonstrated with integrated separations to produce ibuprofen in the laboratory (*18*, *19*). Ley and co-workers have reported on the flow-based preparation of an antimalarial drug, using a combination of solution-based and solid-supported reagents and catalysts (*20*). Collaboration between Novartis and the Massachusetts Institute of Technology resulted in "end-to-end" CM—including in-line separations and production of solid-dose oral drug product—of non-CGMP aliskiren hemifumarate (*21*, *22*). Another flow approach used packed columns in the realm of natural product synthesis (*23*). Our group set out to design a continuous CGMP production method for an active clinical candidate to realize many of the aforementioned benefits under pharmaceutically relevant quality control conditions.

Checkpoint kinase 1 (CHK1) is a multifunctional protein kinase that regulates DNA replication and the repair of damaged DNA. Prexasertib monomesylate monohydrate (**11**, Fig. 1), inhibits the enzymatic activity of CHK1 with a median inhibitory concentration (IC_{50}) < 1 nM in cell-free assays and has been shown to induce DNA damage, as measured by replication catastrophe (*24*–*27*). Prexasertib is being assessed in phase 1b and 2 clinical trials in combination with cytotoxic chemotherapy, targeted agents, and as a monotherapy (*28*) and is the first CHK1 inhibitor to demonstrate objective clinical responses as a monotherapy (*29*). Due to low oral bioavailability, **11** is administered via infusion; hence, appreciable aqueous solubility is desirable for the drug substance. **11** has previously been manufactured by a nine-step route, which was deemed unsuitable for long-term manufacturing due to several hazardous reagents and suboptimal bond disconnections. We designed a distinct seven-step synthesis route amenable to CM (Fig. 1). Concurrently, prexasertib monolactate monohydrate (**12**) was identified as having improved aqueous solubility relative to the mesylate and was targeted for commercialization.

Optimization of a hydrazine condensation reaction in flow

The initial four steps were conducted in batch mode to afford nitrile **7**, the starting material for the CGMP sequence (*30*). Step one involved condensation of **7** with hydrazine to form pyrazole

[1]Small Molecule Design and Development, Lilly Research Laboratories, Eli Lilly and Company, Indianapolis, IN 46285, USA. [2]Technical Services/Manufacturing Science, Eli Lilly and Company, Indianapolis, IN 46285, USA. [3]Technical Services/Manufacturing Science, Eli Lilly and Company, Greenfield, IN 46140, USA. [4]Quality Assurance, Eli Lilly and Company, Dunderrow, Kinsale, County Cork, Ireland. [5]Technical Services/Manufacturing Science, Eli Lilly and Company, Dunderrow, Kinsale, County Cork, Ireland. [6]Process Engineering, Eli Lilly and Company, Dunderrow, Kinsale, County Cork, Ireland. [7]Quality Control, Eli Lilly and Company, Dunderrow, Kinsale, County Cork, Ireland.
*Corresponding author. Email: k_cole@lilly.com

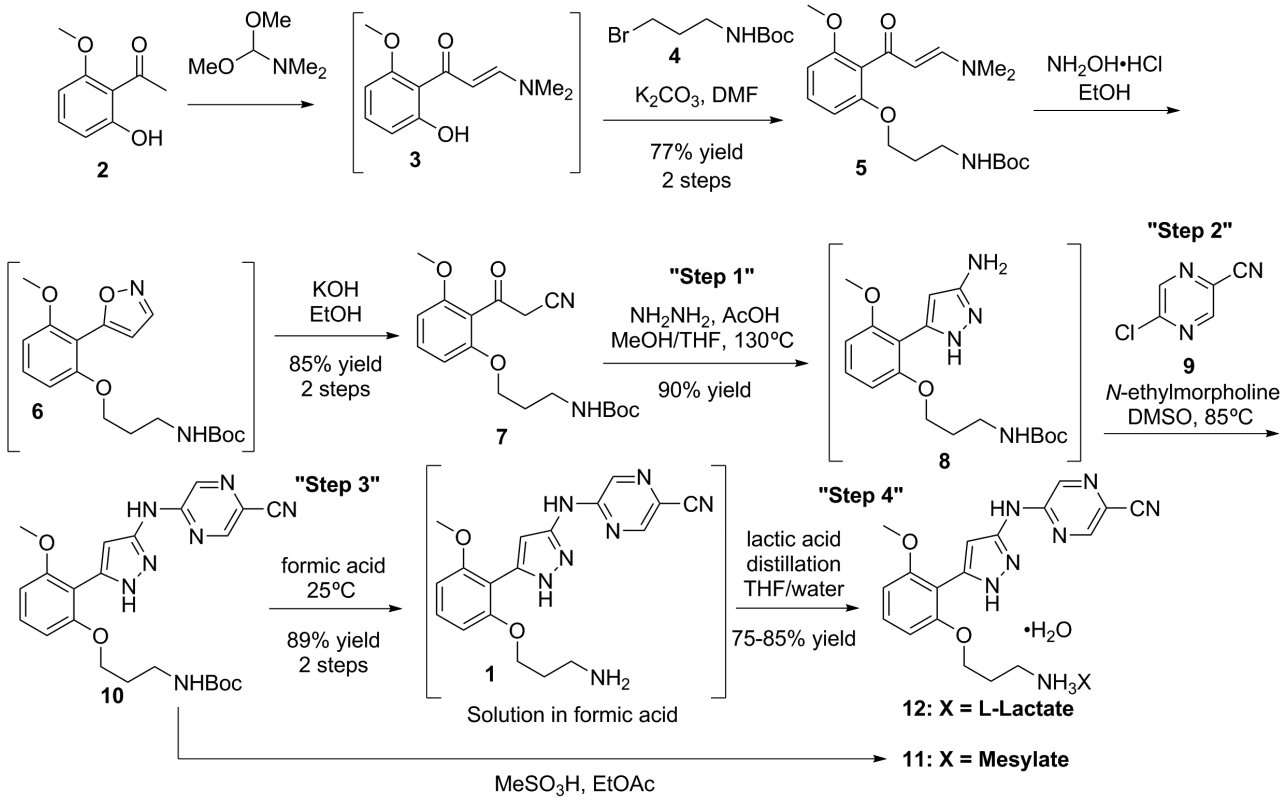

Fig. 1. Continuous manufacturing production route for prexasertib monolactate monohydrate. Brackets indicate nonisolated intermediates. For simplicity, only CGMP steps are assigned a step number. Yields are calculated from production scale. Me, methyl; DMF, *N*,*N*-dimethylformamide; Boc, *tert*-butoxycarbonyl; Et, ethyl; Ac, acetyl; THF, tetrahydrofuran; DMSO, dimethylsulfoxide.

8. In batch mode, this transformation proceeded slowly and required a large molar excess of hazardous hydrazine. Solvents that enabled higher temperatures and faster reaction rates introduced challenges in the isolation and purification of **8** and were avoided. Both **7** and **8** exhibited high solubility in tetrahydrofuran (THF), and superheating the process stream under pressure using small-volume stainless steel pressure reactors improved the reaction rate (*31*). Screening of reaction temperature, stoichiometry, and time was conducted in batch mode, which allows for rapid evaluation of parallel reaction conditions and resource minimization. Batch screening can also help identify potential intermediate or product solubility liabilities, which could result in reactor plugging in flow. In most cases, more upfront work is conducted for the first flow reaction in comparison with a batch reaction. Special care is taken to ensure homogeneous feed, intermediate, and product streams, which may lead to selection of nonstandard reagents or solvents. These studies were quickly translated to flow in a 3.2-ml stainless steel (316L) plug flow reactor (PFR) constructed with tubing of 0.56-mm inner diameter (ID). Further optimization in flow revealed that at 130°C and 500 pounds per square inch gauge, highly pure **8** could be obtained in high yield, using a mean residence time (τ) of 60 min and a slight excess of hydrazine. At production scale (3.4 kg/day of **7**), the PFR volume was 1.4 liters, constructed from 91 m of 4.57-mm-ID tubing, and the reactor was heated within a modified gas chromatography oven (figs. S25 and S26). These conditions were unsuited to batch processing, owing to the high temperature and pressure. Hydrazine can safely be used under these conditions because in the PFR only 20 g of hydrazine was present at any time, as compared with a batch process in which the hazardous reagent can be present in the reactor all at once. Similarly, another benefit of the flow process was the minimization of material at risk, as the reactor contained only 0.49% of the overall production material at any given time. During start-up there was no transition waste cut. All of the reactor outflow was forward-processed because the impact of dilute product in the downstream extraction system was negligible.

Minor impurities were observed in the stream of **8**, and it was necessary to purge residual reagents and perform a solvent exchange. Toluene was added to facilitate a layer separation, and aqueous washing removed hydrazine, acetic acid, and the largest process impurity: deprotected **8**. This impurity was shown to increase at higher temperatures or with prolonged heating. Because pyrazole **8** exhibits some solubility in aqueous media, a continuous countercurrent extraction was developed to minimize product loss (figs. S1 and S27 to S29 and table S1). It was composed of three stages—each with a mixing tank for rapid mass transfer between layers and a static gravity decanter for layer separation—and provided the required purification with minimal product loss (*32*). Hydrazine was controlled to <2 parts per million relative to **8**, and the deprotected impurity could be removed from as much as 5% to less than 1% of the total integrated product distribution detected by high-performance liquid chromatography (HPLC area %) after extraction. Because **8** had tested positive in an Ames mutagenicity assay (*33*) and had poor crystallinity, it was carried forward as a crude solution. Avoiding isolation also afforded increased yield and reduced waste and operational exposure. The extracted product flowed into a surge vessel (*34*) (table S7) that fed the subsequent intermittent-flow (*4*) solvent exchange and enabled continuous operation of the upstream reaction and extraction, despite the intermittent-flow nature of the evaporator.

The solution of **8** was then concentrated to remove THF, methanol, toluene, and water, using an automated 20-liter rotary evaporator (*5*), which was selected over other evaporator types (such as falling film) because it was required for the step-four concentration and could therefore be used twice during the production, reducing the overall equipment cost. During the concentration, dimethylsulfoxide (DMSO) was added to afford the intermediate solution of **8**. The intermittent-flow mode of operation consisted

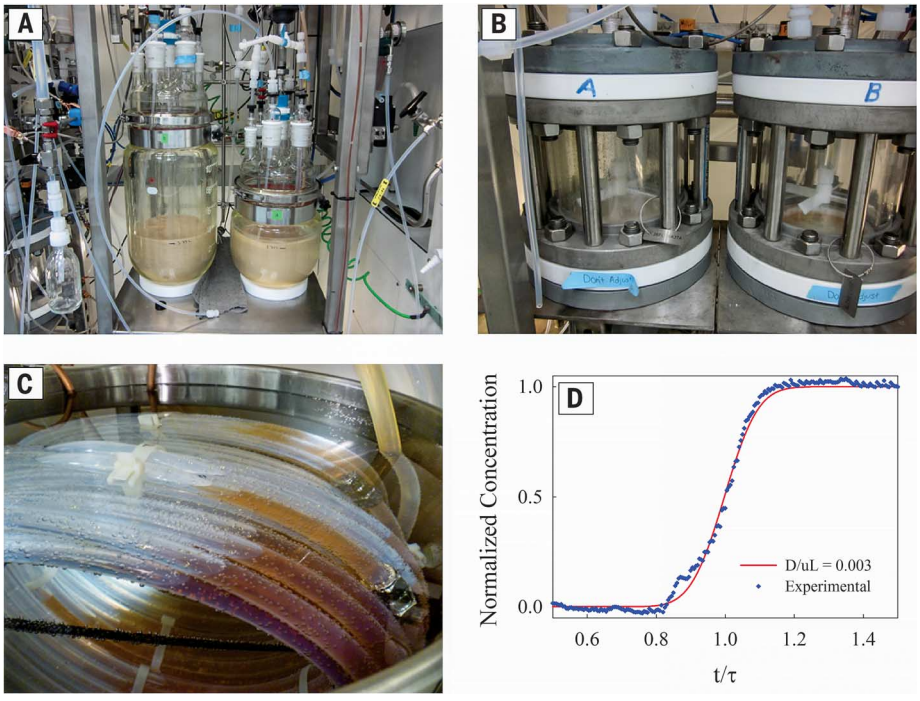

Fig. 2. Experimental apparatus. Photographs of (**A**) mixed-suspension, mixed-product removal vessels (MSMPRs); (**B**) dissolve-off filters; and (**C**) a gas-liquid deprotection plug flow reactor (PFR) with (**D**) observed deprotection reactor output response to an inlet step change (f-curve). See the supplementary materials for details of model fitting. D, dispersion coefficient; u, velocity; L, reactor length; t, elapsed time; τ, mean residence time.

of charging the extracted solution of **8** to the evaporator, removal of the solvents to near dryness under vacuum, and dissolution of the residue in DMSO (table S2 and figs. S30 and S31). No specific thermal stability issues were noted in this concentration, and the maximum processing temperature of 110°C was based on thermal stability data of nitrile **7**. The capability to concentrate to near dryness with a substantial tolerance toward transient solids is a particular advantage of this method, which can minimize waste and processing time. All of the intermittent process flows into and out of the evaporator were fully automated, which integrated solvent exchange into the continuous process. The automated intermittent-flow evaporator was not a truly continuous unit operation, but it was a practical method for incorporating solvent exchange into the middle of an otherwise continuous processing train. The production rate of 3.1 kg/day for **8** was suitable for SVC manufacturing (fig. S39). The concentrated DMSO solution of **8** [30% weight/weight (w/w)] could be directly transferred to the subsequent chemical step but was typically stored and exhibited excellent chemical stability in excess of 60 days.

Nucleophilic substitution and product crystallization protocol

In step two, an S_NAr reaction between **8** and pyrazine **9** (*30*, *35*) provided **10**, with good yield and selectivity. Under optimal conditions, <5 HPLC area % of pyrazole-arylated regioisomers were produced as a 4:1 mixture. Pyrazole **10**, sparingly soluble in most solvents, exhibited solubility in DMSO in excess of 17% (w/w) at ambient temperature. DMSO also provided better chemical reaction rates and reaction profiles compared with other solvents. A base was required to neutralize the HCl by-product, which can cause premature *tert*-butoxycarbonyl (Boc) removal and slow the desired reaction. *N*-Ethylmorpholine (NEM) was selected because NEM and its HCl salt are soluble in DMSO at relevant concentrations, and NEM is minimally reactive with **9**. The reaction was optimized using batch experiments, and assay yields of 90% were typical when a slight excess of **9** was employed in the presence of NEM at temperatures of 70° to 100°C for 1 to 3 hours. The flow reaction was conducted in a low-pressure PFR constructed from inexpensive perfluoroalkoxy (PFA) tubing, which was selected for ease of fabrication and absence of the corrosion concerns associated with metallic tubing. Deliberate fluid mixing before the reactor was required, which was accomplished by an upfront section of narrow-diameter PFA tubing that provided diffusional mixing between the initial mixing tee and the main reactor. At production scale (2.9 kg/day of **10**), the PFR volume was 2.8 liters and consisted of a PFA tube (6.35 mm ID by 91 m) immersed in a heated bath (figs. S32, S33, and S40).

The crude solution of **10** was typically 90 area % by HPLC, and a purification was necessary to remove residual **9**, the regioisomers, low levels of other process impurities, NEM·HCl, and DMSO. An antisolvent crystallization using methanol delivered **10** in high yield and purity; methanol provided for maximum process yield and acceptable slurry viscosity. Other antisolvent options exhibited similar yield with inferior slurry mobility or decreased yield with acceptable mobility. Particle nucleation and crystallization kinetics of this system were rapid and amenable to an SVC process, as the system could achieve the throughput target within the desired fume hood footprint. A viscous slurry formed if too little antisolvent was added, likely on account of the crystal size and habit of **10**, impeding slurry transfer from vessel to vessel. Although this phenomenon is not commonly a barrier to continuous crystallization development, it is not reserved to this case. Other crystallizations with similar morphology, solvent volume, and viscosity would exhibit the same mobility issue. A continuous crystallization process using two mixed-suspension, mixed-product removal vessels (MSMPR) in series overcame this issue (figs. S34 and S35). A custom-built intermittent-flow transfer zone (*5*) was used for slurry movement between vessels and onto one of two parallel automated collection filters. This mode of slurry transfer has been shown to minimize solids fouling that would impede the process; some build-up of solids inside the MSMPRs is typical but did not interfere with the process.

The crystallization was accomplished with a 1-hour τ in each MSMPR (Fig. 2). All methanol was added to the first MSMPR, avoiding a solvent composition that would result in a highly viscous slurry. The slurry from the crystallization was intermittently filtered on one of two automated and agitated single-plate filters (fig. S2). The tandem filters were designed to achieve product filtration, solids washing, partial drying of the solids with nitrogen, and agitated dissolution of the solids with formic acid. The filters were fully automated and required no manual intervention. This eliminated the potential for operator exposure to the solids, as the occupational exposure limit for **10** and **12** is 1 μg/m^3. The filters were controlled by the distributed control system (DCS) and operated in an alternating fashion every hour: While one was actively receiving aliquots of product slurry, the other was engaged in the sequence of washing, drying, dissolution, and cleaning in anticipation of the next cycle.

Owing to the operating mode of the filters and the integrated continuous process, it was necessary to understand the filtration performance of product to ensure that the filtration throughput matched or exceeded the process throughput to avoid interruptions to the adjacent continuous unit operations. Laboratory assessments of cake filtration properties, along with a model to describe gas flows and discrete scheduling operations, enabled calculations of filter idle times as a function of filter size and process throughput. The modeling effort facilitated the development of an optimized operational schedule and ensured that the filter was sized appropriately (each filter pad was 0.018 m^2) with predictable and reliable operating policies, while minimizing the footprint of the automated unit operation (0.37 m^2). The

continuous crystallization of **10** represented the most important element of the impurity control strategy for production of **12**. The purity of the crystallized solids was in excess of 99.8 HPLC area %. Moreover, manual handling and sampling of the dried solids was not required. Small slurry samples were periodically taken from the crystallizers to assess physical properties, supersaturation, and purity. The continuous MSMPRs and intermittent-flow filters provided the impurity rejection of a classical crystallization without the solids handling of a classical isolation.

Step 2 was started with the PFR full with solvent, and the initial outflow was diverted to waste to avoid dilution or dissolution of the slurry in the crystallizer. The measured residence time distribution (RTD) of the PFR was used to determine when the product concentration approached full strength, triggering the switch of PFR outflow into MSMPR1. MSMPR1 was initiated at a solvent composition equal to the combined addition ratio, and the solid content was started at the expected state of control value (*36*). MSMPR2 was started empty to minimize the amount of solid **10** seed needed for start-up.

Deprotection with simultaneous gas and liquid handling

Exposure of **10** to formic acid promoted removal of the Boc protecting group. Addition of formic

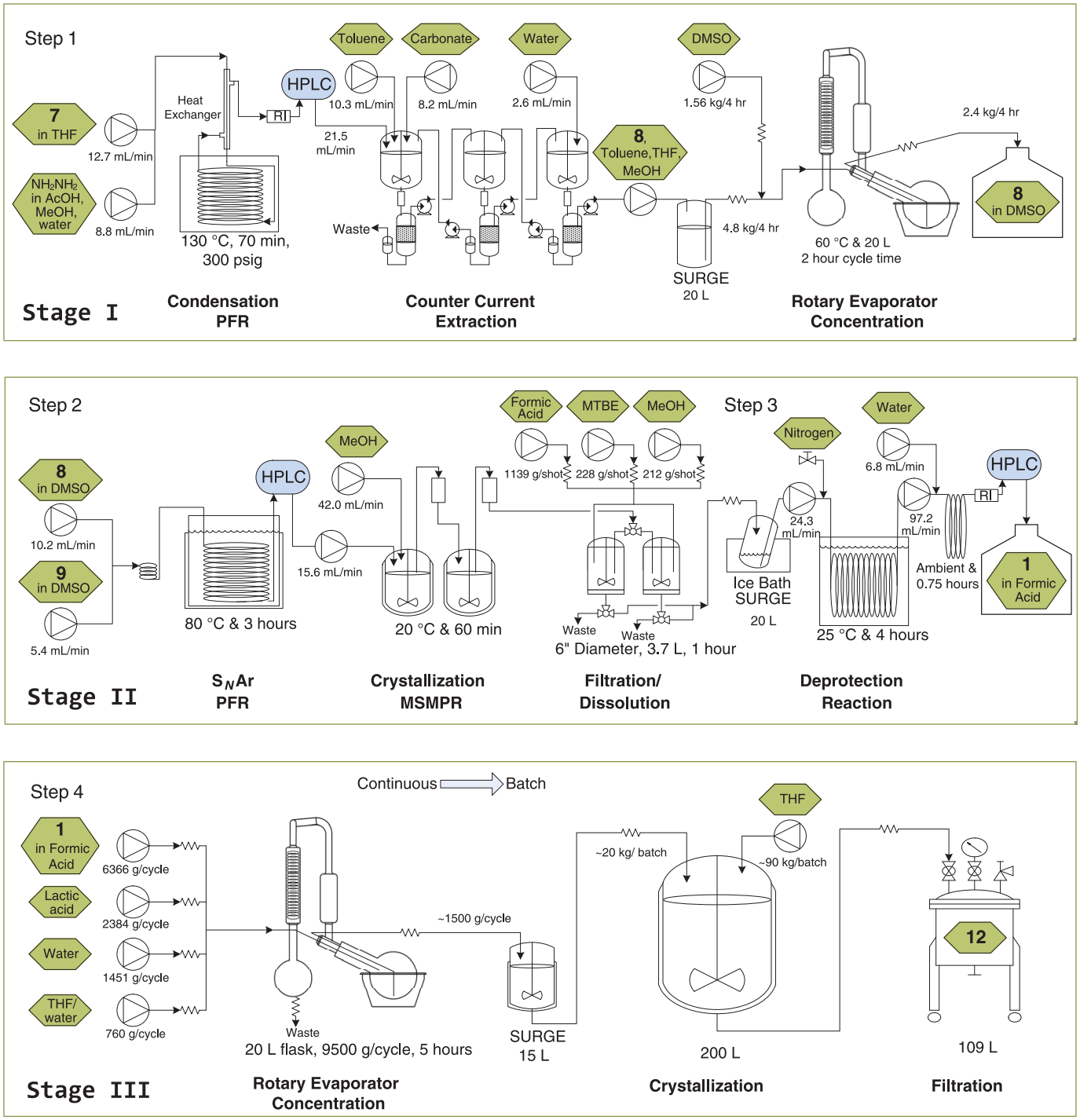

Fig. 3. Continuous CGMP operation for prexasertib monolactate monohydrate. RI, refractive index probe; psig, pounds per square inch gauge; MTBE, methyl *tert*-butyl ether.

acid and mechanical agitation of the solids on the filter provided rapid dissolution, allowing the solution to flow through the filter into a surge vessel maintained at 0° to 5°C, which flowed directly into the step-three reactor. The surge vessel enabled continuous operation in the deprotection step, despite the intermittent nature of the filtration and dissolution. The surge vessel also decoupled steps two and three, allowing for a temporary shutdown of one step without disturbing the other. The step-three deprotection reaction exhibited excellent robustness between 20° and 40°C, with mean residence time of 2 to 6 hours. The wide acceptable processing range afforded good stability in case of process upset or temporary flow stoppage. An improved impurity profile was realized when the gaseous by-products of the deprotection, CO_2 and *iso*-butylene, were removed in situ. A custom vertically oriented PFR reactor was designed to accomplish this (figs. S36 to S38): A coil of 15.9-mm-ID PFA tubing was positioned on its side (like a wheel) and operated 50% filled with liquid and 50% filled with gas (predominately with nitrogen carrier gas). Peristaltic pumps were used to control the flow rate of liquid and gas through the reactor such that the liquid τ was 4 hours and the gas τ was 80 min. Gas bubbled through the liquid on the uphill side of each tube coil, and the downhill side of each tube coil remained almost completely gas-filled because of the gravity flow of the liquid. An outlet pump was used to minimize intermittent surging of liquid from the reactor. Characterization of the reactor revealed plug flow operation with a dispersion number (D/uL, where D is the dispersion coefficient, u is the velocity, and L is the reactor length) of 0.003, which approximates the RTD of 140 equal-volume stirred-tank reactors in series. Water stabilized the product upon refrigerated storage and was added to the reactor outflow. The solution of **1** in aqueous formic acid was stable upon refrigeration for at least 60 days, and any residual **10** converted to **1** upon storage (table S3). Major process impurities observed were the *tert*-butyl carboxamide derived from a Ritter reaction, a labile *tert*-butyl amine, and a formamide of **1**. Release testing was conducted on this product solution, which was held before use in the final isolation. The reactor started filled with liquid formic acid. During the start-up transition, the reactor effluent was diverted to waste for one reactor volume turnover to reduce the amount of dilution before the next flow unit operation, which was an intermittent-flow evaporator. The reactor outflow was not at steady-state operation at the time that the divert valve was switched to forward-process material, but it had been shown that this product solution was acceptable. None of the three PFRs in this continuous train was required to reach steady state; rather, a state of control was achieved before forward-processing material.

Formation of the final lactate salt

In step four, it was necessary to remove formic acid to below 0.8 equivalents relative to the API in the presence of excess lactic acid to enable the isolation of **12**. It was possible to isolate the formate salt and convert it to **12**, but this necessitated an additional isolation of a high-containment solid, and yields were inferior. The addition of eight equivalents of 30% (w/w) lactic acid and concentration using the same automated rotary evaporator described earlier afforded the product as a solution in lactic acid, which could then be crystallized to produce **12** (table S4 and figs. S3 and S4). The concentration step was controlled by time, temperature, pressure, and mass flows. The solvent strip could not be replicated in batch mode because a batch tank cannot achieve the thin film obtained in the rotary evaporator. This was important because elevated impurity formation occurred with extended processing time. After concentration, the oil was diluted with aqueous THF and automatically transferred from the evaporator to a surge vessel, where it gradually accumulated. From the surge vessel, the solution was transferred to the crystallizer for batch crystallization using additional THF as an antisolvent. Batch crystallization was selected because of insufficient time to develop a robust continuous process without undue risk to the likelihood of success. Although polymorphism of **12** itself was not an issue, salt form contamination and hydration state were known areas of concern. Multiple polymorphs of the anhydrous formate salt were possible and were governed by relative formate-to-lactate counterion concentrations. A dilactate salt form exists and could be observed at high lactic acid concentrations. A minimum water concentration was necessary to maintain the hydration state of **12** in the crystallizer, as well as upon drying. During process development, these factors had been examined only in batch mode, which reinforced the decision to use the batch API crystallization at this time. In our experience, many unit operations take a similar amount of time to develop in either batch or flow modes because the data required to design in either mode are similar. In this case, the time to develop the flow process was projected to be longer due to integration of the continuous crystallization with continuous concentration and continuous polish filtration at elevated temperature.

A full process demonstration was conducted in development labs in Indianapolis, Indiana, at the same scale, throughput, and operational schedule as that intended for CGMP production. The ability to conduct development at full scale was enabled by SVC manufacturing and provided a high level of assurance for a successful technology transfer, as scale-dependent operations or process flaws could be identified and remediated before CGMP production. Several of the production equipment sets were fabricated in Indianapolis and shipped to the Lilly CGMP manufacturing plant in Kinsale, Ireland. A discussion of the CGMP equipment qualification strategy can be found in the supplementary materials. The CGMP manufacture was conducted in three stages to minimize risk (Fig. 3). This permitted the solutions of **8** and **1** to be collected

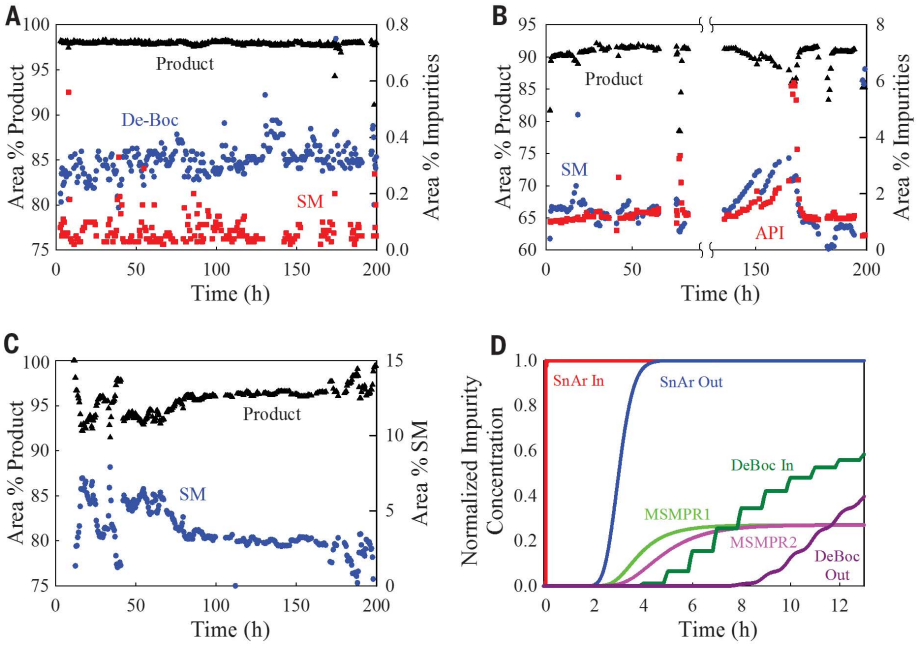

Fig. 4. Process metrics. (**A**) Online HPLC data from step one. (**B**) Online HPLC data from step two. Note the lapse in time due to instrument malfunction, as well as the increase of starting material **8** (SM) and active pharmaceutical ingredient (API) around 150 hours. (**C**) Online HPLC data from step three. (**D**) Residence time distribution (RTD) estimated from the process model for push-in (see supplementary materials for details on RTD calculations). Data from (D) were used to decide when product containers began to be affected by the disturbance. Impurity push-out calculations (fig. S24) were used to determine when the disturbance was no longer affecting product drums.

Table 1. Operational statistics from the CGMP campaign.

Step	1	3	4
Product	**8** (DMSO solution)	**1** (formic acid solution)	**12**
Yield (%)	89.6	88.7	75–85
Purity (HPLC area %)	98.25	99.02–99.07	99.77–99.82
Batches	1	3	5
Total run time (hours)	207	208	290
Product throughput (kg/day)	3.08	2.56	1.99

and stored between steps as discrete fractions, which allowed for extensive release testing to be conducted. The existing facility did not possess adequate fume hood space for the entire process to be conducted simultaneously but is currently being refitted to enable full CGMP SVC production (*37*). Further discussion on capital and operational expenses, as related to SVC manufacturing, is included in the supplementary materials.

Because **12** is administered via infusion, the drug product requires aseptic processing conditions, and it was not deemed practical to attempt integration with drug substance. Standard practice for parenteral API manufacturing is to conduct a final filtration of the process solution for the purposes of product quality assurance. In this case, 0.45-μm filtration was performed on all streams entering the step-four rotary evaporator, as well as all solvent streams entering the batch crystallizer. The API crystallization was conducted in a 200-liter vessel, and the solids were discharged to an agitated filter dryer. The yield from the crystallization varied (75 to 85%) (Table 1) and was determined to correlate with stir time due to the slow growth kinetics of the crystal (tables S3 and S5).

Analytics under CGMP conditions

Key online analytical trends and process modeling output from the CGMP production campaign are shown in Fig. 4. In total, 24 kg of **12** was produced, which amounts to ~114,000 individual doses. Online PAT was heavily used during development to monitor and characterize the processes, and these tools proved crucial during the CGMP production to confirm process health and demonstrate that the process was in a state of control. PAT used during production included online HPLC and refractive index measurement, as well as temperature, pressure, and mass flow rates monitored by the DCS. The online HPLC data were not intended for CGMP decision-making; forward-processing decisions were reached using manual, offline testing. The online PAT was intended to inform minor adjustments to the process parameters to keep the process performance on target. The PAT was not integrated with the DCS, and the system was not designed for feedback control on the basis of the analytical data.

After several days of processing, a disturbance was detected by the online HPLC: The outflow from the step-two PFR began to exhibit elevated levels of pyrazole **8** and API **1**, presumably as **1**·HCl. Under these conditions, **1**·HCl is soluble in DMSO but is poorly rejected in the subsequent crystallization. In most solvent matrices, **1**·HCl is highly insoluble, and any chloride present in the final crystallization results in contamination of **12** with the hydrochloride. Production was paused to allow investigation. It was suspected that the reaction contained insufficient NEM, so samples of the feed solution of **8** were taken for offline testing, and additional NEM was charged to the solution. For restart, the step-three deprotection reactor was initiated first to empty the surge vessel and minimize the spread of affected material. Once the coupling reactor was restarted, the levels of both **1** and **8** returned to a state of control over time. In this instance, had online PAT not been available, the disturbance would likely have gone undetected for a longer period of time, exposing more material to risk. Upon investigation, it was determined that evaporative loss of NEM from the feed stream had occurred over time, resulting in a pH imbalance. Propagation of this disturbance through the system was simulated using a composite flow-sheet model considering the measured or calculated RTDs for each of the individual unit operations in the system (table S6 and figs. S19 to S24). The model clearly illustrated the RTD broadening effect of the crystallizers and surge vessel in the system and aided in making decisions to minimize the duration of the disturbance. The solution of **1** in formic acid was collected in discrete containers, allowing for the segregation of the containers that were affected by the disturbance, and these were treated with an additional filtration before crystallization to remove the insoluble **1**·HCl. The API batches that did not receive this additional filtration exhibited higher chloride levels and turbidity upon dissolution, indicating some level of chloride propagation throughout the production. The detection of the disturbance and decision to pause the reaction were based on the online HPLC data and resulted in a manufacturing deviation, which was resolved upon offline analysis. As SVC manufacturing matures, it will become necessary in some instances for online PAT and associated models to be integrated with the DCS to facilitate real-time forward-processing decisions.

Outlook

By using an integrated continuous process under SVC manufacturing, we succeeded in producing 24 kg of CGMP prexasertib monolactate monohydrate for use in human clinical trials. Eight continuous unit operations were used in series, and four of these operated simultaneously in fume hoods. Recognized benefits of CM included the ability to operate at high temperature in a low-boiling solvent, improved safety for a hazardous reaction, better yield and impurity rejection via countercurrent multistage extraction, improved containment of a highly potent material, the use of a dedicated and disposable equipment set in transparent vessels, efficient solvent stripping with enhanced performance in terms of product stability, elimination of one isolation and elimination of solids handling in another isolation, and increased quality assurance and process understanding provided by online PAT and process automation. A continuous reactor type was developed and deployed, as was a method for in-process filtration and redissolution. We believe that this mode of pharmaceutical manufacturing will become common within the industry within the next decade.

REFERENCES AND NOTES

1. S. Wollowitz, *Drug Dev. Res.* **71**, 420–428 (2010).
2. V. M. Richon, *Hematology* **2013**, 19–23 (2013).
3. A. Gautam, X. Pan, *Drug Discov. Today* **21**, 379–384 (2016).
4. K. P. Cole *et al.*, *Org. Process Res. Dev.* **20**, 820–830 (2016).
5. T. D. White *et al.*, *Org. Process Res. Dev.* **16**, 939–957 (2012).
6. J. S. Srai, C. Badman, M. Krumme, M. Futran, C. Johnston, *J. Pharm. Sci.* **104**, 840–849 (2015).
7. D. M. Roberge *et al.*, *Org. Process Res. Dev.* **12**, 905–910 (2008).
8. E. Palmer, "GSK doubles down on Singapore continuous processing plant," *FiercePharma*, 29 June 2015; www.fiercepharma.com/partnering/gsk-doubles-down-on-singapore-continuous-processing-plant.
9. S. L. Lee *et al.*, *J. Pharm. Innov.* **10**, 191–199 (2015).
10. U.S. Food and Drug Administration (FDA), "FDA perspective on continuous manufacturing," presented at the IFPAC Annual Meeting, Baltimore, MD, 22 to 25 January 2012 (FDA, 2013); www.fda.gov/downloads/AboutFDA/CentersOffices/OfficeofMedicalProductsandTobacco/CDER/UCM341197.pdf.
11. E. Palmer, "FDA urges companies to get on board with continuous manufacturing," *FiercePharma*, 14 April 2016; www.fiercepharma.com/manufacturing/fda-urges-companies-to-get-on-board-continuous-manufacturing.
12. L. X. Yu *et al.*, *AAPS J.* **16**, 771–783 (2014).
13. B. Gutmann, D. Cantillo, C. O. Kappe, *Angew. Chem. Int. Ed.* **54**, 6688–6728 (2015).
14. A. Adamo *et al.*, *Science* **352**, 61–67 (2016).
15. S. A. May *et al.*, *Org. Process Res. Dev.* **16**, 982–1002 (2012).
16. S. A. May *et al.*, *Org. Process Res. Dev.* **20**, 1870–1898 (2016).
17. "Niacin and niacinamide: A commitment to quality" (Lonza, 2015); www.ethorn.com/ssw/files/Lonza.pdf.
18. A. R. Bogdan, S. L. Poe, D. C. Kubis, S. J. Broadwater, D. T. McQuade, *Angew. Chem. Int. Ed.* **48**, 8547–8550 (2009).
19. D. R. Snead, T. F. Jamison, *Angew. Chem. Int. Ed.* **54**, 983–987 (2015).
20. S.-H. Lau *et al.*, *Org. Lett.* **17**, 3218–3221 (2015).
21. S. Mascia *et al.*, *Angew. Chem. Int. Ed.* **52**, 12359–12363 (2013).
22. J. L. Quon *et al.*, *Cryst. Growth Des.* **12**, 3036–3044 (2012).
23. T. Tsubogo, H. Oyamada, S. Kobayashi, *Nature* **520**, 329–332 (2015).
24. C. King *et al.*, *Mol. Cancer Ther.* **14**, 2004–2013 (2015).
25. D. Hong *et al.*, *J. Clin. Oncol.* **34**, 1764–1771 (2016).
26. F. S. Farouz, R. C. Holcomb, R. Kasar, S. S. Myers, U.S. Patent 20110144126 A1 (2011).
27. F. S. Farouz, R. C. Holcomb, R. Kasar, S. S. Myers, WO Patent 2010077758 A1 (2010).
28. ClinicalTrials.gov, LY2606368 [accessed April 2017]; https://clinicaltrials.gov/ct2/results?term=ly2606368&Search=Search.

29. J. Lee *et al*., . *Ann. Oncol.* **27** (suppl. 6), 8550 (2016).
30. Materials and methods are available as supplementary materials.
31. M. O. Frederick *et al*., *Org. Process Res. Dev.* **19**, 1411–1417 (2015).
32. M. D. Johnson *et al*., *Org. Process Res. Dev.* **16**, 1017–1038 (2012).
33. K. Mortelmans, E. Zeiger, *Mutat. Res.* **455**, 29–60 (2000).
34. A. Faanes, S. Skogestad, *Ind. Eng. Chem. Res.* **42**, 2198–2208 (2003).
35. G. Palamidessi, A. Vigevani, F. Zarini, *J. Heterocycl. Chem.* **11**, 607–610 (1974).
36. "Guidance for industry: Quality systems approach to pharmaceutical CGMP regulations" (FDA, 2006); www.fda.gov/downloads/Drugs/.../Guidances/UCM070337.pdf.
37. "Eli Lilly to invest €35m in Kinsale plant," *The Irish Times*, 5 April 2016; www.irishtimes.com/business/health-pharma/eli-lilly-to-invest-35m-in-kinsale-plant-1.2598781.

ACKNOWLEDGMENTS

We thank B. Huff for executive support for CM, J. Buser and M. Embry for nuclear magnetic resonance assistance, W.-M. Sun for process automation programming, and M. Rosemeyer for assistance with Fig. 3. D&M Continuous Solutions constructed the CGMP equipment. We thank the reviewers whose thoughtful suggestions improved the quality of this manuscript. Experimental procedures, ^{1}H and ^{13}C data for new compounds, additional text on materials handling, equipment qualification procedures, capital and operational expenses, detailed yield calculations, equipment operational parameters and automation details, equipment photographs, and modeling information can be found in the supplementary materials.

SUPPLEMENTARY MATERIALS

www.sciencemag.org/content/356/6343/1144/suppl/DC1
Materials and Methods
Supplementary Text
Figs. S1 to S40
Tables S1 to S7
References (*38*, *39*)

1 March 2017; accepted 18 May 2017
10.1126/science.aan0745

Kilogram-scale prexasertib monolactate monohydrate synthesis under continuous-flow CGMP conditions

Kevin P. Cole, Jennifer McClary Groh, Martin D. Johnson, Christopher L. Burcham, Bradley M. Campbell, William D. Diseroad, Michael R. Heller, John R. Howell, Neil J. Kallman, Thomas M. Koenig, Scott A. May, Richard D. Miller, David Mitchell, David P. Myers, Steven S. Myers, Joseph L. Phillips, Christopher S. Polster, Timothy D. White, Jim Cashman, Declan Hurley, Robert Moylan, Paul Sheehan, Richard D. Spencer, Kenneth Desmond, Paul Desmond, and Olivia Gowran

Science, **356** (6343), .
DOI: 10.1126/science.aan0745

Go with the flow in drug manufacturing

Although many commodity chemicals are manufactured using continuous flow techniques, pharmaceuticals are still mostly produced in large single batches. Cole *et al.* report a protocol for the small-volume continuous preparation of multi-kilogram quantities of a cancer drug candidate, prexasertib monolactate monohydrate, under current good manufacturing practices. Advantages of the approach include safer handling of hazardous reagents and intermediates, as well as yield and selectivity improvements in both the reaction and purification stages. Concurrent analytical monitoring also facilitated rapid trouble-shooting during the manufacturing process.

Science, this issue p. 1144